



Published in final edited form as:

Dev Dyn. 2013 May ; 242(5): 550–559. doi:10.1002/dvdy.23928.

Tbx1 is required for second heart field proliferation in zebrafish

Kathleen Nevis^{1,2}, Pablo Obregon^{1,2}, Conor Walsh^{1,2}, Burcu Guner-Ataman^{1,2}, C. Geoffrey Burns^{1,2,3,*}, and Caroline E. Burns^{1,2,3,*}

¹Cardiovascular Research Center, Massachusetts General Hospital, Harvard Medical School, Charlestown, MA 02129, USA

²Harvard Medical School, Boston, MA 02115

³Harvard Stem Cell Institute, Cambridge, MA 02138, USA

Abstract

Background—The mammalian outflow tract (OFT) and primitive right ventricle arise by accretion of newly differentiated cells to the arterial pole of the heart tube from multi-potent progenitor cells of the second heart field (SHF). While mounting evidence suggests that the genetic pathways regulating SHF development are highly conserved in zebrafish, this topic remains an active area of investigation.

Results—Here, we extend previous observations demonstrating that zebrafish *tbx1* (*van gogh*, *vgo*) mutants show conotruncal defects consistent with a conserved role in SHF-mediated cardiogenesis. Surprisingly, we reveal through double *in situ* analyses that *tbx1* transcripts are excluded from cardiac progenitor cells or differentiated cardiomyocytes, suggesting a non-autonomous role in SHF development. Further, we find that the diminutive ventricle in *vgo* animals results from a 25% decrease in cardiomyocyte numbers that occurs subsequent to heart tube stages. Lastly, we report that although SHF progenitors are specified in the absence of Tbx1, they fail to be maintained due to compromised SHF progenitor cell proliferation.

Conclusion—These studies highlight conservation of the Tbx1 program in zebrafish SHF biology.

Keywords

tbx1; zebrafish; heart; second heart field; cardiac

Introduction

In higher vertebrates cardiac crescent cells of the first heart field (FHF) generate the primitive heart tube, which is elongated at both poles by late differentiation of second heart field (SHF) progenitors in pharyngeal mesoderm (Vincent and Buckingham, 2010). At the arterial pole, SHF precursors give rise to new myocardial segments that become the future right ventricle and outflow tract (OFT). Anomalies in OFT development comprise ~30% of congenital heart defects (Srivastava and Olson, 2000) and often result from hemizygous microdeletions in a 3 Mb region on chromosome 22q11.2 (Jerome and Papaioannou, 2001; Lindsay et al., 2001; Merscher et al., 2001). This genomic disruption results in a variable constellation of congenital malformations and cognitive impairments known collectively as DiGeorge Syndrome (DGS). Among the most life-threatening phenotypes are cardiovascular (CV) anomalies, such as Tetralogy of Fallot and Interrupted Aortic Arch, that appear to arise

from reduced expression of *TBX1*, a gene in the typically deleted region required for cardiac neural crest and SHF development (Jerome and Papaioannou, 2001; Lindsay et al., 2001; Merscher et al., 2001; Yagi et al., 2003). Despite the prevalence and severity of CV malformations in the DGS population, ~20% of genetically affected individuals lack any detectable cardiovascular pathology (Ryan et al., 1997). This observation underscores the profound influence of genetic and/or environmental modifiers over the DGS phenotype and reveals the complexity of the requirement for *TBX1* in CV development. As such, a more detailed understanding of the molecular mechanisms by which *TBX1* influences OFT development are essential.

Much of our understanding of how *TBX1* influences CV development comes from gene expression and inactivation studies in the mouse (Aggarwal and Morrow, 2008; Parisot et al., 2011; Scambler, 2010). Murine *Tbx1* is expressed in tissues that form the pharyngeal system - including pharyngeal surface ectoderm, pharyngeal endoderm, and pharyngeal mesoderm, which contains SHF progenitors (Chapman et al., 1996; Garg et al., 2001; Jerome and Papaioannou, 2001; Lindsay et al., 2001; Merscher et al., 2001; Vitelli et al., 2002a). In regards to the heart, cre/loxP lineage tracing of *Tbx1*⁺ cells showed substantial contribution to the inferior myocardial wall and endothelium of the OFT and some contribution to the myocardium at the base outlet of the RV, consistent with *Tbx1* expression in a subset of SHF precursors (Huynh et al., 2007; Xu et al., 2004). Loss of function analyses revealed that homozygous *Tbx1* neonates die at birth from severe craniofacial and CV malformations, the latter of which include the loss of the pharyngeal apparatus (pharyngeal arches, pouches, and clefts), OFT hypoplasia, and ventricular septal defects (Jerome and Papaioannou, 2001; Lindsay et al., 2001; Merscher et al., 2001). It has been proposed that *TBX1* provides a pro-proliferation signal to SHF progenitors (Chen et al., 2009; Liao et al., 2008; Xu et al., 2004; Zhang et al., 2006b) that is likely mediated, at least in part, by FGF8 (Abu-Issa et al., 2002; Brown et al., 2004; Hu et al., 2004; Park et al., 2006; Vitelli et al., 2010; Vitelli et al., 2002b; Zhang et al., 2006b). This idea is supported by the ability of *TBX1* to activate an *Fgf8* enhancer in cell culture (Hu et al., 2004) and by genetic interaction studies between *Tbx1* and *Fgf8* for OFT development *in vivo* (Brown et al., 2004; Vitelli et al., 2010; Vitelli et al., 2002b; Zhang et al., 2006b).

Why only a fraction of patients hemizygous for a deletion in the *TBX1* containing region present with DGS while others have no observable abnormalities is not understood. Moreover, the spectrum of defects in affected DGS individuals suggests the existence of genetic or environmental modifiers, most of which are not known. The zebrafish model organism offers distinct strategies for identifying such modifiers, such as forward genetic or small molecule based screening. Despite being comprised of only two cardiac chambers, the zebrafish heart is partially derived from a SHF population (de Pater et al., 2009; Hami et al., 2011; Lazic and Scott, 2011; Zhou et al., 2011) that expresses *nkx2.5* (Lazic and Scott, 2011; Zhou et al., 2011), *mef2cb* (Himits et al., 2012; Lazic and Scott, 2011), and *itbp3* (Zhou et al., 2011). Cre/loxP lineage tracing demonstrated that approximately half of the single ventricular chamber and entire OFT is derived via late differentiation and accretion of SHF progenitors following heart tube formation (Zhou et al., 2011). Impairment of SHF-mediated cardiogenesis results in loss of ventricular cardiomyocytes that normally comprise the distal portion of the chamber and loss or diminution of Elastin2⁺ (Eln2⁺) smooth muscle precursor cells of the OFT.

The genetic programs regulating SHF biology in the zebrafish appear largely conserved with that of higher vertebrates. Using small molecule, morpholino, or genetic means of inhibition, FGF (de Pater et al., 2009; Lazic and Scott, 2011; Marques et al., 2008), BMP (Hami et al., 2011), Hedgehog (Hami et al., 2011), and TGFβ (Zhou et al., 2011) signaling have all been implicated as critical SHF pathways in zebrafish. *Islet1* is arguably the best known SHF

marker in mice. Despite recent reports suggesting conserved expression of *isll* in zebrafish SHF progenitors (Hami et al., 2011; Witzel et al., 2012), *isll*^{-/-} mutants show normal arterial pole development (de Pater et al., 2009). Thus, while evidence of genetic conservation between zebrafish and mammalian SHF-mediated cardiogenesis is mounting, this topic is still an active area of investigation.

In regards to *tbx1*, an initial study in zebrafish showed that *tbx1* null embryos (*van gogh*, *vgo*) (Piotrowski et al., 2003) have an undersized ventricle, a small Eln2+ smooth muscle component of the outflow tract, and impaired migration of dye-labeled pharyngeal cells into the heart tube (Hami et al., 2011). Taken together, these observations suggest preliminarily that zebrafish Tbx1 is required for SHF development. However, a more comprehensive characterization of the *vgo* cardiac phenotype is required to determine the degree to which Tbx1 function is conserved. Thus, we sought to confirm and extend initial observations suggesting that Tbx1 function is required for zebrafish SHF development as in mice and presumably humans.

Here, we characterized *tbx1* expression in relation to cardiac progenitors and differentiated cardiomyocytes in zebrafish and analyzed *tbx1/vgo* null embryos for molecular and morphological evidence of SHF perturbations. Unexpectedly, we found that *tbx1* expression appears non-overlapping with cardiac progenitor cell (CPC) markers of the first or second heart fields or differentiated cardiomyocytes that comprise the early zebrafish heart tube. However, *vgo* mutant ventricles show a clear diminution in size. We discovered that this reduction in ventricular chamber size is due to an approximately 25% decrease in cardiomyocyte numbers that occurs subsequent to linear heart tube establishment. This finding demonstrates that FHF development occurs normally in the absence of Tbx1 function, but that SHF development is specifically disrupted. Further, we discovered that the SHF defect in *vgo* mutants is caused by compromised SHF progenitor cell proliferation. Overall, our data suggest that the *tbx1* pathway is conserved in zebrafish for SHF-mediated cardiogenesis.

Results

Although the developmental expression pattern of zebrafish *tbx1* has been reported previously (Kochilas et al., 2003; Piotrowski et al., 2003; Zhang et al., 2006a), we sought to characterize the location of *tbx1* transcripts relative to cardiac markers during the initial phases of zebrafish cardiogenesis. First, we performed double *in situ* hybridization prior to early myocardial differentiation with *tbx1* and the conserved cardiac progenitor marker, *nkx2.5*, which is expressed in both the first and second heart fields. At the 8 somite-stage [8ss; 13 hours post-fertilization (hpf)], *tbx1* transcripts are located medial (Fig. 1A,B) and dorsal (Fig. 1A,D) to *nkx2.5*⁺ CPCs. Interestingly, *fgf8a* transcripts were reported to have a similar dorsomedial relationship with *nkx2.5* at similar developmental stages (Reifers et al., 2000). Cross-section analysis provided further evidence that *tbx1* expression is non-overlapping with *nkx2.5* (Fig. 1C). Next, we examined the localization of *tbx1* transcripts relative to a cardiomyocyte marker, *cardiac myosin light chain 2* (*cmlc2*; also called *myl7*) (Yelon et al., 1999) and a SHF marker latent TGF-beta binding protein-3 (*Itbp3*). At 16ss (17hpf), *cmlc2* transcripts mark FHF-derived myocardial cells in the anterior lateral plate mesoderm (ALPM) (de Pater et al., 2009; Lazic and Scott, 2011). At this stage, *tbx1* transcripts were observed lateral to the medially migrating *cmlc2*⁺ cardiomyocytes of the heart forming region (Fig. 1E). Similarly at 23ss (20.5hpf), *tbx1* transcripts were readily visible in the developing pharyngeal arches (Piotrowski et al., 2003), but absent from *cmlc2*⁺ cells that comprise the cardiac cone, a precursor to the linear heart tube in zebrafish (Fig. 1F). At the same developmental stage, *Itbp3* expression commenced in SHF progenitors adjacent to the cardiac cone, but failed to overlap spatially with *tbx1* (Fig. 1G).

Finally, after establishment of the linear heart tube (24hpf), *tbx1* transcripts were absent from the heart tube proper (Fig. 1H) and the arterial pole of the heart tube inhabited by SHF progenitor cells (Fig. 1H, inset) (Hami et al., 2011; Lazic and Scott, 2011; Zhou et al., 2011). Taken together, these data suggest that zebrafish *tbx1* transcripts are non-overlapping with CPC markers of the first or second heart fields or differentiated cardiomyocytes that comprise the early zebrafish heart tube.

To determine if zebrafish embryos devoid of *tbx1* display evidence of defective cardiogenesis, we analyzed embryos homozygous for the *tbx1* null alleles, *van gogh^{tu285}* (*vgot^{tu285}*) and *van gogh^{tu208}* (*vgot^{tu208}*), which produce indistinguishable embryonic phenotypes (Piotrowski et al., 2003; Piotrowski and Nusslein-Volhard, 2000). To visualize cardiogenesis in absence of *tbx1*, we crossed the *vgot^{tu285}* allele with our previously described Tg(*nkx2.5:ZsYellow*)^{*tb7*} line that reports yellow fluorescence in *nkx2.5*+ cells (henceforth called *nkx2.5:ZsY*) (Zhou et al., 2011). Consistent with a previous report (Hami et al., 2011), we observed a diminutive ventricle in *vgot* mutants compared to controls at 72hpf (Fig. 2A–D), a timepoint following SHF-mediated myocardial accretion (de Pater et al., 2009; Lazic and Scott, 2011; Zhou et al., 2011). This size difference could be due to a decrease in the number of ventricular cardiomyocytes or equivalent numbers of ventricular cells that are smaller and more densely organized. To distinguish between these alternatives, we quantified the number of cardiomyocytes in each chamber of control and *vgot^{tu285}* mutant embryos at 72hpf using a transgenic strain in which cardiomyocyte nuclei express DsRed2 fluorescent protein (Mably et al., 2003). From this analysis, we learned that *vgot* embryos display no alterations in the number of atrial cells but exhibit an approximately 25% decrease in the number of ventricular cardiomyocytes compared to controls (Fig. 2E–G). Moreover, OFT smooth muscle precursors that are marked by Elastin2 (*Eln2*) (Miao et al., 2007) were severely diminished or absent in *vgot* embryos compared to control siblings (Fig. 2H–J). Together, these data demonstrate that the small ventricle observed in *vgot* mutants is a result of a ventricular cardiomyocyte deficit and suggest that *tbx1* is essential to build the arterial pole of the zebrafish heart.

A decrease in the number of ventricular cardiomyocytes could arise from a defect in FHF-mediated cardiogenesis. Therefore, we first compared the spatial and temporal expression of cardiac markers at the cone stage (23ss/20.5hpf), a timepoint prior to SHF-mediated myocardial accretion, between *vgot^{tu285}* and sibling embryos. At 23ss, *nkx2.5:ZsY* reporter fluorescence (Fig. 3A,B) and *ventricular myosin heavy chain (vmhc)* transcripts (Fig. 3C,D), which highlight differentiated FHF-derived ventricular cardiomyocytes and undifferentiated SHF progenitors (Lazic and Scott, 2011; Zhou et al., 2011), appeared grossly normal in *vgot* animals. Next, we quantified the number of cardiomyocytes in the linear heart tube of control and *vgot* embryos that derive from early-differentiating FHF cells. We found that although the heart tube of *vgot* animals appeared somewhat misshapen compared to their sibling controls, the total number of cardiomyocytes was similar (Fig. 3E–G). These data provide conclusive evidence that FHF-derived cardiogenesis is unaffected in *vgot* mutants, formally demonstrating that the ventricular phenotype observed is not due to compromised FHF development.

Recently, we and others have demonstrated that zebrafish cardiogenesis relies on a second (or secondary) heart field (SHF) that resides in pharyngeal mesoderm and accretes myocardium to the arterial pole of the linear heart tube (de Pater et al., 2009; Hami et al., 2011; Lazic and Scott, 2011; Zhou et al., 2011). The molecular signature of the zebrafish SHF to date is *nkx2.5*, *mef2cb*, and *ltbp3*. *ltbp3* is the most specific marker of the SHF because it overlaps only partially with differentiated myocardium of the heart tube (Zhou et al., 2011) whereas *nkx2.5* (Lazic and Scott, 2011; Zhou et al., 2011) and *mef2cb* (Himits et al., 2012; Lazic and Scott, 2011) label the SHF and the heart tube. To determine if the

ventricular deficit in *vgo*^{tu285} mutants is a result of perturbations in *Itbp3* expression, we performed *in situ* hybridization using an *Itbp3* riboprobe at progressive developmental stages. At 23ss (20.5hpf), when *Itbp3* transcripts are first visualized by *in situ* analyses, we learned that *Itbp3* expression was properly initiated in *vgo* embryos (Fig. 4A,B). However, at linear heart tube stages (24hpf), *Itbp3* transcripts were no longer detected in SHF progenitors at the arterial pole in *vgo* mutants (Fig. 4 C,D). We confirmed the absence of SHF precursors at heart tube stages in *vgo*^{tu208} embryos using a complementary approach that relies on the fluorescent reporter transgenic strains *Tg(nkx2.5:ZsY)* and *Tg(cmlc2:GFP)*. To distinguish the two fluorophores by confocal microscopy, double fluorescent immunohistochemistry was performed to highlight *cmlc2*⁺ differentiated cardiomyocytes in green and *nkx2.5*⁺ SHF progenitors and differentiated ventricular cardiomyocytes in red. Although a distinct *nkx2.5*⁺ population of SHF progenitors could be easily visualized at the arterial pole of the heart tube at 24–26 hpf in control embryos, this population was absent in *vgo* mutants (Fig. 4E,F). Together, these data suggest that *Tbx1* is required for SHF progenitor cell maintenance, but is dispensable for their initial specification.

To elucidate the cellular mechanisms underlying the *vgo* SHF phenotype, we evaluated mutants soon after cardiac cone stages for cellular defects in the extra-cardiac population of *nkx2.5*⁺ SHF cells at the arterial pole. First, we used TUNEL (terminal deoxynucleotidyl transferase biotin-dUTP nick end-labeling) labelling to highlight apoptotic cells in control and *vgo*^{tu285} mutants carrying the *nkx2.5:ZsY* transgene. Although TUNEL⁺ apoptotic cells were observed throughout the bodies of both control and *vgo* embryos, no TUNEL⁺ cells were detected in the *ZsY*⁺ SHF domain (data not shown). Next, we used the thymidine analog EdU to examine the proliferative state of *nkx2.5:ZsY*⁺ SHF cells at the arterial pole. Specifically, embryos were pulsed with 5-ethynyl-2'-deoxyuridine (EdU) at 20ss (19 hpf) and collected at 26ss (22hpf) for processing using Click-iT Alexa-555 along with antibody staining for ZsYellow. We detected extensive proliferation throughout the bodies of both *vgo*^{tu285} and sibling controls (Fig. 5A,B). Interestingly, we observed abundant proliferative *ZsY*⁺ cells that predominantly localized to the arterial pole/SHF region of the cardiac cone (Fig. 5C,E). However, while cardiac development appeared similar between *vgo* and sibling controls (Fig 5A,B; insets), a significant decrease in the number of proliferative EdU⁺ SHF progenitors was observed in *vgo* mutants (Fig. 5C–E). These findings support a model in which *Tbx1* stimulates proliferation or self-renewal of *Itbp3*⁺; *nkx2.5*⁺ SHF progenitors to maintain the CPC pool as new myocardium is accreted to the linear heart tube. Based on this model, we speculate that loss of *Tbx1* results in a premature depletion of undifferentiated CPCs from the SHF.

Discussion

Because SHF perturbations are predicted to be common causes of conotruncal malformations in patients, studies designed to decipher the molecular regulation of SHF biology are significant. Specifically, any gene implicated in SHF development becomes a candidate that, when mutated, may cause OFT-related congenital heart defects. Mounting evidence suggests that the genetic pathways regulating SHF development are highly conserved in zebrafish. Here, we extend previous observations showing that zebrafish *tbx1* mutants show conotruncal defects consistent with a role in SHF development. These studies serve to further solidify the use of the zebrafish model organism for discovery based approaches that may uncover new and potentially clinically relevant genes important for arterial pole development.

Deciphering the tissue-specific roles of *TBX1* in mammalian OFT morphogenesis has been extremely complex due in part to the high degree of interaction between the *Tbx1*-

expressing pharyngeal endoderm and pharyngeal mesoderm, the latter of which contains SHF progenitors. While conditional loss-of-function studies have yielded valuable information, the interpretations have been clouded by cre-mediated recombination in both tissue compartments. For example, although deletion of *Tbx1* in the *Nkx2.5* expression domain results in OFT hypoplasia, recombination occurs in the pharyngeal endoderm, pharyngeal mesoderm, and SHF (Xu et al., 2005; Xu et al., 2004). In another study, Arnold et al. showed that deletion of *Tbx1* in the *Foxg1+* pharyngeal endoderm results in severe OFT defects that resemble those occurring in *Tbx1*^{-/-} nulls (Arnold et al., 2006). Although *Foxg1*-mediated recombination was reported to be limited to pharyngeal endoderm in this study (Arnold et al., 2006), Zhang et al. observed additional *Foxg1*-induced cre activity in pharyngeal mesoderm when examining recombination on a different genetic background (Zhang et al., 2005). Thus, the specific interplay between the pharyngeal endoderm and mesoderm in regards to TBX1 function remains unclear.

The most compelling argument that TBX1 functions cell non-autonomously for SHF development in the mouse was shown through mosaic analyses (Xu et al., 2004). Specifically, *Tbx1*^{-/-} cells were mixed with wild-type cells to generate embryos of mixed genetic origin. In these mice, *Tbx1*^{-/-} cells contributed to the SHF, showed no proliferative disadvantage, and were accreted at the same frequency as wild-type cells to the developing OFT. Interestingly, inactivation of *Tbx1* in *Mesp1+* mesoderm results in severe OFT defects that can be rescued by mesodermal restoration of *Tbx1* (Zhang et al., 2006b). Although these data show a strict requirement for *Tbx1* in the mesoderm, *Mesp1* is expressed rather broadly leaving open the possibility that *Tbx1* is required in a mesodermal population distinct from the SHF. Thus, the outcome of these lineage-specific inactivation/reactivation experiments remains consistent with those from the chimera analyses that demonstrated a non-autonomous role for TBX1 in SHF-mediated OFT formation.

Our studies in zebrafish show that *Tbx1* is required for SHF proliferation and, based on its expression pattern, most likely acts cell non-autonomously. Although our *in situ* analyses are unable to definitively exclude *tbx1* expression in medial *nkx2.5+* cells in the heart forming region that may represent SHF progenitors, the domains appear separate. Moreover, we failed to observe transcripts in the region occupied by SHF progenitors at cardiac cone or heart tube stages. Our observations coupled with previous reports showing *tbx1* transcripts in the pharynx (Piotrowski et al., 2003) makes it tempting to speculate that perhaps the role of *Tbx1* in pharyngeal tissues has been conserved in zebrafish for OFT development. However, chimera analyses to determine autonomy in OFT development and cre/loxP-mediated genetic lineage tracing of *tbx1*-expressing cells in zebrafish will be required to appreciate the complete *tbx1* expression profile and tissue derivatives during cardiac development.

Although *tbx1* does not appear to be expressed in SHF progenitors in zebrafish, our data and that of Hami et al. show that *Tbx1* is required for SHF development. Experimental evidence garnered from *Itbp3* cre/loxP lineage tracing (Zhou et al., 2011) and a photoconversion assay that measures the timing of cardiomyocyte differentiation (Lazic and Scott, 2011) suggests that approximately 40–50% of the ventricular chamber is derived from SHF progenitors following heart tube formation. However, our ventricular cardiomyocyte counts in *tbx1* mutants revealed only a 25% reduction. This outcome could be explained several ways. It is possible that only 25% of the ventricle is derived from SHF cells and that our previous cre/loxP lineage tracing overestimated contribution as *Itbp3* expression partially overlaps with differentiated cardiomyocytes at the end of the heart tube. Alternatively, because *Itbp3* expression is initiated in *tbx1* null animals, it is possible that there is only a partial myocardial deficit in *vgo* animals. Another explanation, which is consistent with its role in the mouse (Parisot et al., 2011), is that *Tbx1* is required for proper development of a sub-

domain within a larger SHF. As new SHF markers and lineage traces emerge in zebrafish, a better understanding of the full complement of cardiovascular derivatives of the SHF will be revealed, ultimately aiding our understanding of mutant phenotypes and gene function.

Experimental Procedures

Zebrafish lines and maintenance

Zebrafish embryos, larvae, and adults were produced, grown and maintained according to standard protocols approved by the Institutional Animal Care and Use Committees of Massachusetts General Hospital. Ethical approval was obtained from the Institutional Animal Care and Use Committees of Massachusetts General Hospital. The previously published (Piotrowski et al., 2003; Piotrowski et al., 1996; Schilling et al., 1996) *vgo*^{tu285} and *vgo*^{tu208} mutant *tbx1* alleles were used in this study. The *vgo*²⁸⁵ and *vgo*²⁰⁸ alleles of *tbx1* contain a C → T and an A → T transition at nucleotide positions 364 and 879 respectively, each creating premature stop codons. Transgenic strains *Tg(cmlc2::DsRed-nuc)* (Mably et al., 2003), *Tg(nkx2.5::ZsYellow)* (Zhou et al., 2011) and *Tg(cmlc2::GFP)* (Burns et al., 2005) were described previously.

Double in situ hybridization, immunohistochemistry, and cryosectioning

Single and double *in situ* hybridization was performed as described (Thisse et al., 1993), with digoxigenin-labeled antisense RNA probes to *Itbp3* (EcoRI/Sp6), *nkx2.5* (EcoRI/T7), *tbx1* (EcoRI/T7), *vmhc* (EcoRI/T3), and fluorescein-labeled antisense RNA probes to *cmlc2* (NotI/T7) and *tbx1*. For cryo-sections, stained embryos were washed in PBS and embedded in 1.2% agarose in a 5% sucrose solution. Embedded embryos were placed in 30% sucrose solution overnight at 4° C. Agarose blocks were covered with Optimal Cutting Temperature compound (OCT) (Tissue-Tek) and 50µm sections were taken using Leica CM 3050 S cryostat. Immunohistochemistry was performed as described (Zhou et al., 2011), using primary antibodies anti-GFP mouse mono-clonal (1:50; Santa Cruz Biotechnology, Santa Cruz, CA), anti-RCFP rabbit polyclonal pan (1:50; Clontech, Mountain View, CA), anti-dsRed rabbit polyclonal (1:50; Clontech, Mountain View, CA), muscle-specific MF20 (1:50; University of Iowa, Iowa City, IA), Elastin-2 (1:1000; Fred Keeley) and secondary antibodies Alexa Fluor 555 goat anti-rabbit IgG_{2b}, Alexa Fluor 488 goat anti-mouse IgG_{2b} and Alexa Fluor 546 goat anti-mouse IgG_{2b} (all 1:200; Invitrogen, Carlsbad, CA).

Bright Field, Fluorescence and Confocal microscopy

Confocal imaging was performed as described previously (Zhou et al., 2011) on a LS5 confocal microscope (Zeiss) using a 40× water immersion objective. ImageJ (v1.43U; National Institute of Health, USA) software was used to count cardiomyocyte (CM) nuclei in Z-stack confocal images. Statistical significance for CM counts was determined using unpaired Student's t-test. Bright field and fluorescent microscopy was performed with a 10x objective on an Eclipse 80i microscope (Nikon, Melville, NY) using a Retiga 2000R camera (Q-imaging, Surrey, BC Canada) and NIS-Elements AR 3.00 imaging software (Nikon).

TUNEL and Click-iT Edu staining

TUNEL (terminal deoxynucleotidyl transferase biotin-dUTP nick end-labeling) was performed as described previously (Zhou et al., 2011). Briefly, *Tg(nkx2.5::ZsYellow)* *vgo*²⁸⁵ mutant and control embryos were collected at 23ss and fixed overnight at 4° C in 4% paraformaldehyde before being transferred to 100% methanol and stored at -20° C. Embryos were rehydrated in methanol/PBST series, permeabilized with proteinase K and subjected to a TUNEL assay via the *In Situ* Cell Death Detection Kit, TMR red (Roche Applied Science) according to the manufacturer's instructions. Proliferation experiments were performed as

previously described (Mahler et al., 2010) using the Click-iT EdU imaging kit (Invitrogen). Briefly, embryos were incubated on ice for 30 minutes in 10mM 5-ethynyl-2'-deoxyuridine (EdU), rinsed 3 times in embryo medium, and chased for 3 hours at 28°C. Immunofluorescent staining with anti-rCFP (Alexa-488) and Click-iT-Alexa-555 was performed and embryos were analyzed using confocal microscopy.

Acknowledgments

We thank L. Zon and I. Scott for providing zebrafish strains; J Holzschuh for providing a detailed Click-iT EdU labeling protocol; Fred Keeley for providing Elastin2 anti-serum, and the Developmental Studies Hybridoma Bank under the auspices of the NICHD and maintained by the University of Iowa, Department of Biological Sciences, Iowa City, IA 52242, for providing the MF20 antibody. This work was supported by awards from the National Institutes of Health to K.N. (5F32HL110627), the American Heart Association to B.G.-A. (10POST4170037), the American Heart Association (Grant in Aid no. 10GRNT4270021) and the National Heart Lung and Blood Institute (5R01HL096816) to C.G.B., and the Harvard Stem Cell Institute (Young Investigator Award and Cardiovascular Program Award), National Heart Lung and Blood Institute (5R01HL111179) and the March of Dimes Foundation (1-FY12-467) to C.E.B.

References

- Abu-Issa R, Smyth G, Smoak I, Yamamura K, Meyers EN. Fgf8 is required for pharyngeal arch and cardiovascular development in the mouse. *Development*. 2002; 129:4613–4625. [PubMed: 12223417]
- Aggarwal VS, Morrow BE. Genetic modifiers of the physical malformations in velo-cardio-facial syndrome/DiGeorge syndrome. *Dev Disabil Res Rev*. 2008; 14:19–25. [PubMed: 18636633]
- Arnold JS, Werling U, Braunstein EM, Liao J, Nowotschin S, Edelmann W, Hebert JM, Morrow BE. Inactivation of *Tbx1* in the pharyngeal endoderm results in 22q11DS malformations. *Development*. 2006; 133:977–987. [PubMed: 16452092]
- Brown CB, Wenning JM, Lu MM, Epstein DJ, Meyers EN, Epstein JA. Cre-mediated excision of *Fgf8* in the *Tbx1* expression domain reveals a critical role for *Fgf8* in cardiovascular development in the mouse. *Dev Biol*. 2004; 267:190–202. [PubMed: 14975726]
- Burns CG, Milan DJ, Grande EJ, Rottbauer W, MacRae CA, Fishman MC. High-throughput assay for small molecules that modulate zebrafish embryonic heart rate. *Nat Chem Biol*. 2005; 1:263–264. [PubMed: 16408054]
- Chapman DL, Garvey N, Hancock S, Alexiou M, Agulnik SI, Gibson-Brown JJ, Cebra-Thomas J, Bollag RJ, Silver LM, Papaioannou VE. Expression of the T-box family genes, *Tbx1-Tbx5*, during early mouse development. *Dev Dyn*. 1996; 206:379–390. [PubMed: 8853987]
- Chen L, Fulcoli FG, Tang S, Baldini A. *Tbx1* regulates proliferation and differentiation of multipotent heart progenitors. *Circ Res*. 2009; 105:842–851. [PubMed: 19745164]
- de Pater E, Clijsters L, Marques SR, Lin YF, Garavito-Aguilar ZV, Yelon D, Bakkens J. Distinct phases of cardiomyocyte differentiation regulate growth of the zebrafish heart. *Development*. 2009; 136:1633–1641. [PubMed: 19395641]
- Garg V, Yamagishi C, Hu T, Kathiriyai IS, Yamagishi H, Srivastava D. *Tbx1*, a DiGeorge syndrome candidate gene, is regulated by sonic hedgehog during pharyngeal arch development. *Dev Biol*. 2001; 235:62–73. [PubMed: 11412027]
- Hami D, Grimes AC, Tsai HJ, Kirby ML. Zebrafish cardiac development requires a conserved secondary heart field. *Development*. 2011; 138:2389–2398. [PubMed: 21558385]
- Himits Y, Pan L, Walker C, Dowd J, Moens CB, Hughes SM. Zebrafish *Mef2ca* and *Mef2cb* are essential for both first and second heart field cardiomyocyte differentiation. *Dev Biol*. 2012
- Hu T, Yamagishi H, Maeda J, McAnally J, Yamagishi C, Srivastava D. *Tbx1* regulates fibroblast growth factors in the anterior heart field through a reinforcing autoregulatory loop involving forkhead transcription factors. *Development*. 2004; 131:5491–5502. [PubMed: 15469978]
- Huynh T, Chen L, Terrell P, Baldini A. A fate map of *Tbx1* expressing cells reveals heterogeneity in the second cardiac field. *Genesis*. 2007; 45:470–475. [PubMed: 17610275]

- Jerome LA, Papaioannou VE. DiGeorge syndrome phenotype in mice mutant for the T-box gene, Tbx1. *Nat Genet.* 2001; 27:286–291. [PubMed: 11242110]
- Kochilas LK, Potluri V, Gitler A, Balasubramanian K, Chin AJ. Cloning and characterization of zebrafish *tbx1*. *Gene Expr Patterns.* 2003; 3:645–651. [PubMed: 12972000]
- Lazic S, Scott IC. Mef2cb regulates late myocardial cell addition from a second heart field-like population of progenitors in zebrafish. *Dev Biol.* 2011; 354:123–133. [PubMed: 21466801]
- Liao J, Aggarwal VS, Nowotschin S, Bondarev A, Lipner S, Morrow BE. Identification of downstream genetic pathways of Tbx1 in the second heart field. *Dev Biol.* 2008; 316:524–537. [PubMed: 18328475]
- Lindsay EA, Vitelli F, Su H, Morishima M, Huynh T, Pramparo T, Jurecic V, Ogunrinu G, Sutherland HF, Scambler PJ, et al. Tbx1 haploinsufficiency in the DiGeorge syndrome region causes aortic arch defects in mice. *Nature.* 2001; 410:97–101. [PubMed: 11242049]
- Mably JD, Mohideen MA, Burns CG, Chen JN, Fishman MC. Heart of glass regulates the concentric growth of the heart in zebrafish. *Curr Biol.* 2003; 13:2138–2147. [PubMed: 14680629]
- Mahler J, Filippi A, Driever W. DeltaA/DeltaD regulate multiple and temporally distinct phases of notch signaling during dopaminergic neurogenesis in zebrafish. *The Journal of neuroscience : the official journal of the Society for Neuroscience.* 2010; 30:16621–16635. [PubMed: 21148001]
- Marques SR, Lee Y, Poss KD, Yelon D. Reiterative roles for FGF signaling in the establishment of size and proportion of the zebrafish heart. *Dev Biol.* 2008; 321:397–406. [PubMed: 18639539]
- Merscher S, Funke B, Epstein JA, Heyer J, Puech A, Lu MM, Xavier RJ, Demay MB, Russell RG, Factor S, et al. TBX1 is responsible for cardiovascular defects in velo-cardio-facial/DiGeorge syndrome. *Cell.* 2001; 104:619–629. [PubMed: 11239417]
- Miao M, Bruce AE, Bhanji T, Davis EC, Keeley FW. Differential expression of two tropoelastin genes in zebrafish. *Matrix Biol.* 2007; 26:115–124. [PubMed: 17112714]
- Parisot P, Mesbah K, Theveniau-Ruissy M, Kelly RG. Tbx1, subpulmonary myocardium and conotruncal congenital heart defects. *Birth Defects Res A Clin Mol Teratol.* 2011; 91:477–484. [PubMed: 21591244]
- Park EJ, Ogden LA, Talbot A, Evans S, Cai CL, Black BL, Frank DU, Moon AM. Required, tissue-specific roles for Fgf8 in outflow tract formation and remodeling. *Development.* 2006; 133:2419–2433. [PubMed: 16720879]
- Piotrowski T, Ahn DG, Schilling TF, Nair S, Ruvinsky I, Geisler R, Rauch GJ, Haffter P, Zon LI, Zhou Y, et al. The zebrafish van gogh mutation disrupts *tbx1*, which is involved in the DiGeorge deletion syndrome in humans. *Development.* 2003; 130:5043–5052. [PubMed: 12952905]
- Piotrowski T, Nusslein-Volhard C. The endoderm plays an important role in patterning the segmented pharyngeal region in zebrafish (*Danio rerio*). *Dev Biol.* 2000; 225:339–356. [PubMed: 10985854]
- Piotrowski T, Schilling TF, Brand M, Jiang YJ, Heisenberg CP, Beuchle D, Grandel H, van Eeden FJ, Furutani-Seiki M, Granato M, et al. Jaw and branchial arch mutants in zebrafish II: anterior arches and cartilage differentiation. *Development.* 1996; 123:345–356. [PubMed: 9007254]
- Reifers F, Walsh EC, Leger S, Stainier DY, Brand M. Induction and differentiation of the zebrafish heart requires fibroblast growth factor 8 (*fgf8/acerebellar*). *Development.* 2000; 127:225–235. [PubMed: 10603341]
- Ryan AK, Goodship JA, Wilson DI, Philip N, Levy A, Seidel H, Schuffenhauer S, Oechsler H, Belohradsky B, Prieur M, et al. Spectrum of clinical features associated with interstitial chromosome 22q11 deletions: a European collaborative study. *J Med Genet.* 1997; 34:798–804. [PubMed: 9350810]
- Scambler PJ. 22q11 Deletion Syndrome: A Role for TBX1 in Pharyngeal and Cardiovascular Development. *Pediatr Cardiol.* 2010
- Schilling TF, Piotrowski T, Grandel H, Brand M, Heisenberg CP, Jiang YJ, Beuchle D, Hammerschmidt M, Kane DA, Mullins MC, et al. Jaw and branchial arch mutants in zebrafish I: branchial arches. *Development.* 1996; 123:329–344. [PubMed: 9007253]
- Srivastava D, Olson EN. A genetic blueprint for cardiac development. *Nature.* 2000; 407:221–226. [PubMed: 11001064]

- Thisse C, Thisse B, Schilling TF, Postlethwait JH. Structure of the zebrafish *snail1* gene and its expression in wild-type, spadetail and no tail mutant embryos. *Development*. 1993; 119:1203–1215. [PubMed: 8306883]
- Vincent SD, Buckingham ME. How to make a heart: the origin and regulation of cardiac progenitor cells. *Curr Top Dev Biol*. 2010; 90:1–41. [PubMed: 20691846]
- Vitelli F, Lania G, Huynh T, Baldini A. Partial rescue of the *Tbx1* mutant heart phenotype by *Fgf8*: genetic evidence of impaired tissue response to *Fgf8*. *J Mol Cell Cardiol*. 2010; 49:836–840. [PubMed: 20807544]
- Vitelli F, Morishima M, Taddei I, Lindsay EA, Baldini A. *Tbx1* mutation causes multiple cardiovascular defects and disrupts neural crest and cranial nerve migratory pathways. *Hum Mol Genet*. 2002a; 11:915–922. [PubMed: 11971873]
- Vitelli F, Taddei I, Morishima M, Meyers EN, Lindsay EA, Baldini A. A genetic link between *Tbx1* and fibroblast growth factor signaling. *Development*. 2002b; 129:4605–4611. [PubMed: 12223416]
- Witzel HR, Jungblut B, Choe CP, Crump JG, Braun T, Dobрева G. The LIM Protein *Ajuba* Restricts the Second Heart Field Progenitor Pool by Regulating *Isl1* Activity. *Dev Cell*. 2012; 23:58–70. [PubMed: 22771034]
- Xu H, Cerrato F, Baldini A. Timed mutation and cell-fate mapping reveal reiterated roles of *Tbx1* during embryogenesis, and a crucial function during segmentation of the pharyngeal system via regulation of endoderm expansion. *Development*. 2005; 132:4387–4395. [PubMed: 16141220]
- Xu H, Morishima M, Wylie JN, Schwartz RJ, Bruneau BG, Lindsay EA, Baldini A. *Tbx1* has a dual role in the morphogenesis of the cardiac outflow tract. *Development*. 2004; 131:3217–3227. [PubMed: 15175244]
- Yagi H, Furutani Y, Hamada H, Sasaki T, Asakawa S, Minoshima S, Ichida F, Joo K, Kimura M, Imamura S, et al. Role of *TBX1* in human del22q11.2 syndrome. *Lancet*. 2003; 362:1366–1373. [PubMed: 14585638]
- Yelon D, Horne SA, Stainier DY. Restricted expression of cardiac myosin genes reveals regulated aspects of heart tube assembly in zebrafish. *Dev Biol*. 1999; 214:23–37. [PubMed: 10491254]
- Zhang L, Zhong T, Wang Y, Jiang Q, Song H, Gui Y. *TBX1*, a DiGeorge syndrome candidate gene, is inhibited by retinoic acid. *Int J Dev Biol*. 2006a; 50:55–61. [PubMed: 16323078]
- Zhang Z, Cerrato F, Xu H, Vitelli F, Morishima M, Vincentz J, Furuta Y, Ma L, Martin JF, Baldini A, et al. *Tbx1* expression in pharyngeal epithelia is necessary for pharyngeal arch artery development. *Development*. 2005; 132:5307–5315. [PubMed: 16284121]
- Zhang Z, Huynh T, Baldini A. Mesodermal expression of *Tbx1* is necessary and sufficient for pharyngeal arch and cardiac outflow tract development. *Development*. 2006b; 133:3587–3595. [PubMed: 16914493]
- Zhou Y, Cashman TJ, Nevis KR, Obregon P, Carney SA, Liu Y, Gu A, Mosimann C, Sondalle S, Peterson RE, et al. Latent TGF-beta binding protein 3 identifies a second heart field in zebrafish. *Nature*. 2011

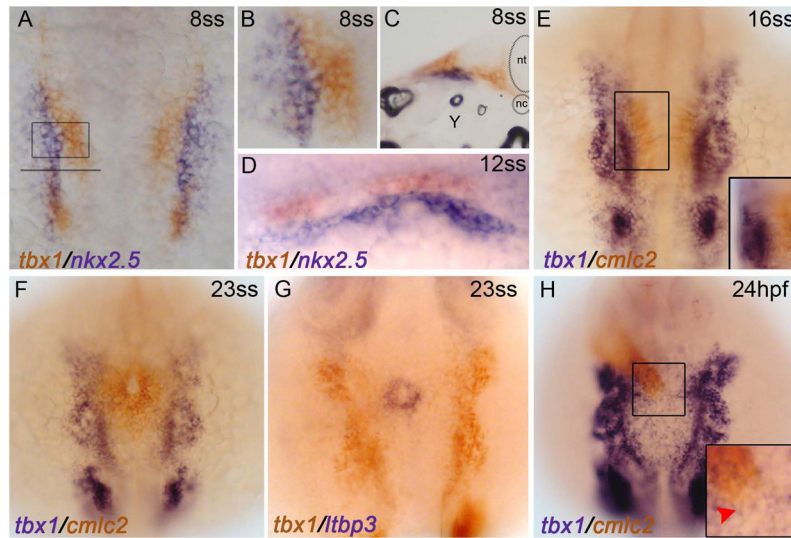


Figure 1. *tbx1* transcripts fail to co-localize with cardiac cells during heart field or heart tube stages

Whole-mount double *in situ* hybridization. (A–D) *tbx1* (red) and *nkx2.5* (blue) transcripts are non-overlapping during heart field stages (8 somite stage). (A) Flat mount, dorsal view, anterior up, 10X magnification. (B) 20X magnification of the ALPM (boxed region from A) (C) Transverse cryo-section, 20X magnification of the ALPM (location of section shown by the solid line in A) (D) Dorso-lateral view showing that *tbx1*-expressing cells lie dorsal to *nkx2.5*-expressing CPCs at the 12ss. (E,F) *tbx1*⁺ cells are lateral to medially migrating *cmlc2*⁺ cardiomyocytes at 16ss and 23ss. (G) *tbx1*⁺ cells are lateral to *ltp3*⁺ SHF progenitors at 20.5hpf/23ss. Dorsal view, anterior up. (H) At 24hpf, the linear heart tube lies dorsal to the *tbx1* expression domain. Dorsal view, anterior up. 10X magnification. (inset) 20X magnification of boxed region from F. *tbx1* is not expressed at the end of the linear heart tube where SHF progenitors reside (red arrowhead).

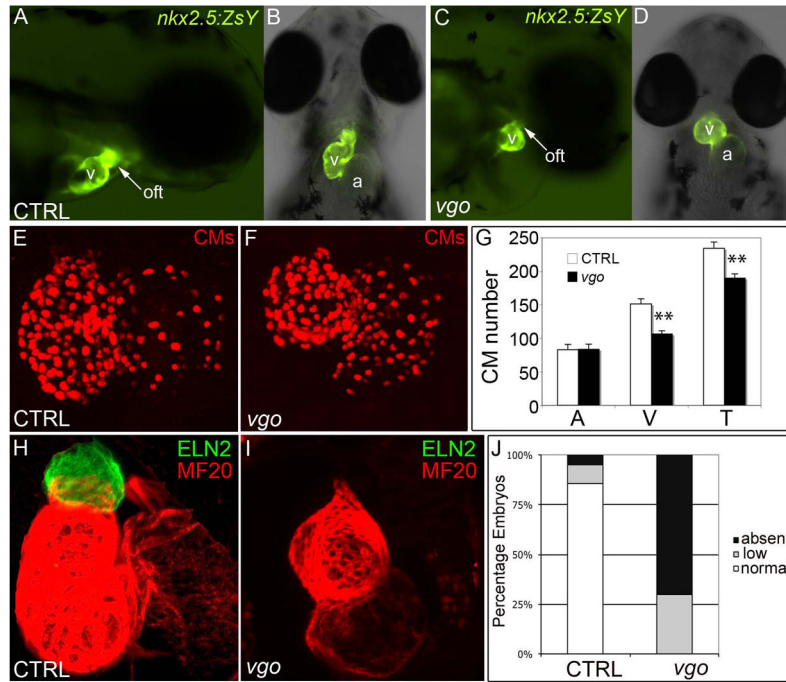


Figure 2. *tbx1* mutants have diminutive ventricles caused by decreased cardiomyocyte numbers and diminished OFT smooth muscle
(A–D) Fluorescent microscopy images of *Tg(nkx2.5:ZsYellow)* control and *vgo* embryos; 10X magnification. At 72hpf, the ventricular chamber and OFT appears small in *vgo* (C, D) compared to control (A,B). A,C; lateral view, anterior right. B,D; ventral view, anterior up. **(E,F)** Flattened confocal images of 72hpf cardiomyocyte (CM) nuclei in *Tg(cmlc2::DsRed^{nuc})* control (E) and *vgo* (F) hearts. **(G)** Graph depicting the average number of CMs at 72hpf in control (n=4) and *vgo* (n=4) embryos. Asterisks indicate statistical significance as determined using unpaired students T-test. Error bars represent +/- s.e.m. Atrial CM numbers remain unchanged ($P=0.47$), while ventricular and total CM numbers are significantly lower in *vgo* mutants ($P=0.00008$ and 0.0002 , respectively). **(H,I)** Flattened confocal images following double immunofluorescence at 72 hpf to visualize OFT smooth muscle precursors (Eln2; green) and chamber cardiomyocytes (MF20; red) in control (n=21; H) and *vgo* (n=20; I) embryos. **(J)** Graph depicting the percentage of control or *vgo* embryos with normal (n), reduced (r), or absent (a) Eln2 staining.

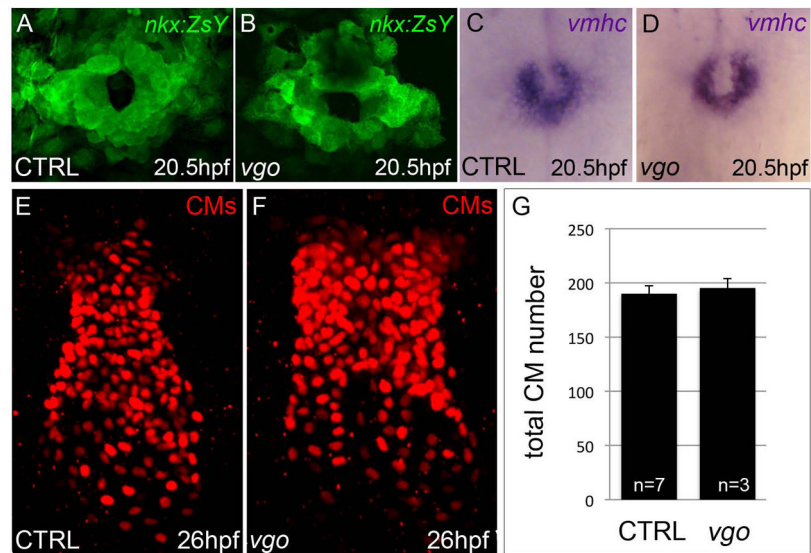


Figure 3. Cardiac progenitors within the heart forming region are specified in *tbx1* mutants and differentiate appropriately into ventricular cardiomyocytes
(A,B) Flattened confocal images of *Tg(nkx2.5::ZsYellow)* control (n=37; A) and *vgo* (n=14; B) embryos at 20.5hpf/23somite-stage (ss). **(C,D)** Whole-mount *in situ* hybridization of *vmhc* at 20.5hpf/23ss in both control (n=16; C) and *vgo* (n=16; D) embryos. **(E,F)** Flattened confocal images following immunofluorescence at 26hpf to visualize DsRed+ nuclei in control (E) and *vgo* (F) embryos. Dorsal view, Anterior up in all images. **(G)** Graph depicting the average number of CMs at 26hpf in control (n=7) and *vgo* (n=3) embryos.

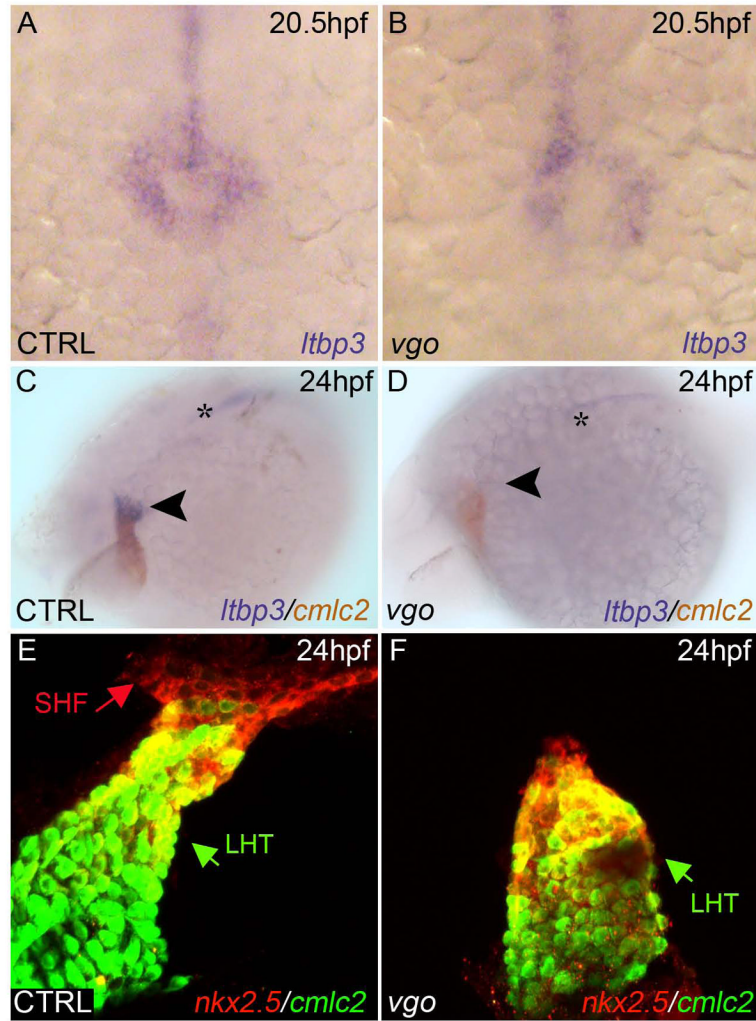


Figure 4. *tbx1* is required for SHF progenitor cell maintenance

(A–B) *ltbp3* was observed via whole-mount *in situ* hybridization at 20.5hpf/23ss in control (A) and *vgo* (B) embryos (n>12). Dorsal view, anterior down. 20X Magnification. (C, D) Whole-mount double *in situ* hybridization at 26 hpf shows *ltbp3*⁺ (blue) cells at the arterial pole (arrowhead) of the *cmlc2*⁺ (red) heart tube in control embryos. *ltbp3* expression is drastically reduced (21%) or absent (79%) at the arterial pole of *vgo* hearts (n=14). Asterisk indicates *ltbp3* expression within the notochord. (E, F) Double transgenic *Tg(nkx2.5::ZsYellow); Tg(cmlc2::GFP)* control (E) and *vgo* (F) embryos co-immunostained with GFP antibody (anti-GFP, green) and ZsYellow antibody (anti-RCFP, red) at 26 hpf. The future atrial segment of the linear heart tube (LHT, green arrow) expresses *cmlc2* alone (green), while the future proximal ventricular myocardium co-expresses *cmlc2* and *nkx2.5* (yellow). Non-myocardial *nkx2.5*⁺ second heart field (SHF) progenitors (red arrow) can be visualized in control animals (n=8), but are lacking in *vgo* mutants (n=7).

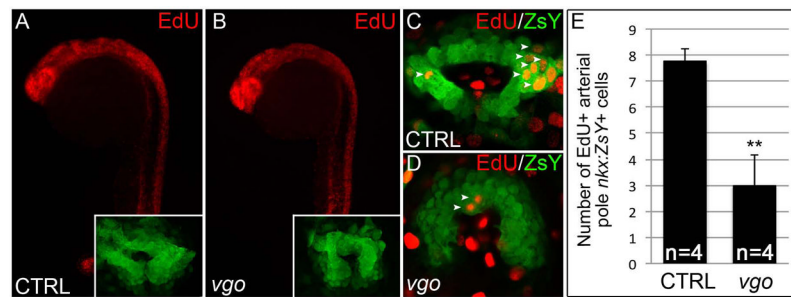


Figure 5. SHF progenitor cells fail to proliferate in the absence of Tbx1

(A–D) Click-iT EdU labeling in *Tg(nkx2.5:ZsYellow)* *vgo* and control siblings. (A–B) Fluorescent microscopy images of EdU+ cells (red) in control (A) and *vgo* (B) embryos. 10X magnification, anterior up, dorsal right. Insets show flattened confocal images of ZsY+ cells at the arterial pole (C–D) Composite of two confocal sections showing EdU+ cells (red) within the ZsYellow+ (green) SHF (white arrowheads). (E) Graph depicting the total number of EdU+ cells in the entire confocal stack in control (n=4) and *vgo* (n=4) embryos.